NUREG/CR-1066
HEDL-TME 79-43

DYNAMIC ANALYSIS TO ESTABLISH NORMAL SHOCK AND VIBRATION OF RADIOACTIVE MATERIAL SHIPPING PACKAGES

QUARTERLY PROGRESS REPORT
APRIL 1, 1979 - JUNE 30, 1979

Hanford Engineering Development Laboratory

Available from

GPO Sales Program
Division of Technical Information and Document Control
U.S. Nuclear Regulatory Commission
Washington, D.C. 20555

and

National Technical Information Service
Springfield, Virginia 22161

DISCLAIMER

NUREG/CR-1066
HEDL-TME 79-43
RT

DYNAMIC ANALYSIS TO ESTABLISH NORMAL SHOCK AND VIBRATION OF RADIOACTIVE MATERIAL SHIPPING PACKAGES

QUARTERLY PROGRESS REPORT
APRIL 1, 1979 - JUNE 30, 1979

Hanford Engineering Development Laboratory

S. R. Fields
S. J. Mech

October 1979

HANFORD ENGINEERING DEVELOPMENT LABORATORY
Operated by Westinghouse Hanford Company
P.O. Box 1970 Richland, WA 99352
A Subsidiary of Westinghouse Electric Corporation
Prepared for the U.S. Nuclear Regulatory Commission
under Interagency Agreement DOE EY-76-C-14-2170
NRC FIN No. B2263

NUREG/CR-1066
HEDL-TME 79-43
RT

DYNAMIC ANALYSIS TO ESTABLISH NORMAL SHOCK AND VIBRATION OF RADIOACTIVE MATERIAL SHIPPING PACKAGES

Quarterly Progress Report
April 1, 1979 - June 30, 1979

S. R. Fields
S. J. Mech

ABSTRACT

This report represents work performed at the Hanford Engineering Development Laboratory operated by Westinghouse Hanford Company, a subsidiary of Westinghouse Electric Corporation, for the Nuclear Regulatory Commission, under Department of Energy Contract No. DE-AC14-76FF02170. It describes technical progress made during the reporting period by Westinghouse Hanford Company and supporting contractors. Functions were developed to characterize the behavior of rail cars and their draft gears when the draft gears bottom out. Response variables from the CARDT and CARDS simulation models are compared with experimental data in both the time and frequency domains using Theil's Inequality Coefficients.

ACKNOWLEDGEMENTS

The authors wish to acknowledge the excellent work of Gary Ray who wrote the FFT (Fast Fourier Transform) program algorithm, and Helen Carlson who transformed the FFT program, the TIC (Theil's Inequality Coefficient) program, and a specially constructed plotting routine, into a chain of post-processors to be used with the cask-rail car simulation models.

CONTENTS

FIGURES

TABLES

DYNAMIC ANALYSIS TO ESTABLISH NORMAL SHOCK AND VIBRATION OF RADIOACTIVE MATERIAL SHIPPING PACKAGES

Quarterly Progress Report
April 1, 1979 - June 30, 1979

SUMMARY OF PROGRESS

1. DEVELOP DYNAMIC MODEL

Car to car characterization functions were developed to characterize the behavior of rail cars and their draft gears during the "solid" or bottomed out state of the draft gears. Separate versions of these functions were installed in the CARDT (Cask Rail Car Dynamic Simulator Test) model and the CARDS (Cask Rail Car Dynamic Simulator) model. The improved models were then used to simulate actual experiments.

The CARDT model was used to simulate a 6-mile/hour impact test between two gravel-loaded hopper cars, and calculated coupler force and other response variables were compared with the corresponding actual data recorded during the test. Good agreement was obtained between calculated and experimental results (see Section 3. VALIDATE MODEL).

The CARDS model was used to simulate Test 3 of the cask-rail car humping tests conducted at the Savannah River Laboratories in July and August 1978. Reasonably good agreement between calculated and experimental values of the coupler forces and calculated and experimental values of the horizontal forces between the cask and the rail car was obtained. However, further modification of the characterization function is required to duplicate a secondary peak in the experimental force vs time curves.

2. DATA COLLECTION AND REDUCTION

Recent efforts to read the reduced experimental data into the Boeing Computer Sciences (BCS) Univac computer system were successful. This allows access to both the experimental and corresponding calculated data files for comparison using two coupled post-processing programs for model validation (see Section 3. VALIDATE MODEL).

Efforts to recover data on Tests 1, 2 and 3, whose timing tracks were lost during transcription, have not been successful. Sandia Laboratories replaced these data with copies of their data on BCS compatible media.

3. VALIDATE MODEL

A measure of how well the CARDT model simulates the behavior of an actual hammer car-anvil car system was obtained by quantitatively comparing calculated coupler forces, relative displacements of the cars' centers of gravity, relative velocities, and relative accelerations with those recorded during a 6-mile/hour impact between two 70-ton hopper cars loaded with gravel. Quantitative comparisons were made using Theil's inequality coefficients for each of the response variables listed, and Theil's multiple inequality coefficient for the simultaneous comparison of all the response variables. The final value of the multiple coefficient is 0.106, measured on a scale from 0 (perfect agreement) to 1 (poor agreement).

Two post-processing programs were developed and linked together to evaluate the performance of the CARDT and CARDS models by comparison of calculated and experimental response variables in both the time and frequency domains. The first program developed was FFT (Fast Fourier Transform). FFT maps response variables from the time domain into the frequency domain. The second program developed was TIC (Theil's Inequality Coefficient). TIC computes both the two-variable and multiple inequality coefficients of response variables in both the time and frequency domains.

INTRODUCTION

This study was initiated in October, 1977 as stated in previous progress reports. The objective of this study is to determine the extent to which the shocks and vibrations experienced by radioactive material shipping packages during normal transport conditions are influenced by, or are sensitive to, various structural parameters of the transport system (i.e., package, package supports, and vehicle). The purpose of this effort is to identify those parameters which significantly affect the normal shock and vibration environments so as to provide the basis for determining the forces transmitted to radioactive material packages. Determination of these forces will provide the input data necessary for a broad range of package-tiedown structural assessments.

Progress on this study from April 1, 1979 to June 30, 1979 will now be discussed.

PROGRESS TO DATE

This study is divided into six tasks as discussed in previous progress reports. Progress on each of these tasks will now be discussed.

1. DEVELOP DYNAMIC MODEL

Car to car characterization functions have been developed to characterize the behavior of rail cars and their draft gears during the "solid" state of the draft gears. The "solid" state of a draft gear refers to that state after bottoming out when the draft gear behaves as a solid beam. This is in contrast to the draft gear's "active" state which is the normal condition before the draft gear spring has reached its limit of travel. A characterization function defines a pseudo spring constant or resistance function for the draft gear for its "solid" state which accounts for dissipation of a portion of the total kinetic energy of the system due to cargo shifting and/or deformation of the cargo or rail car during this state. The spring constant defined is unique in that it increases gradually at first while the cargo shifts or deforms easily, but then rises sharply as the cargo compresses or stiffens. An upper limit is imposed on the spring constant during compression which represents near total compaction of the cargo. Energy dissipation due to crushing and deformation of the cargo during the "solid" state is simulated by removing a large fraction of the potential energy stored in the spring before the draft gear rebounds or recovers at zero relative kinetic energy of the two coupled cars.

A car to car characterization function was first developed during this reporting period for the CARDT (Cask Rail Car Dynamic Simulator Test) model, the simple cask-rail car coupler subsystem model described in Reference 1. The characterization function was then expanded and installed in the CARDS (Cask Rail Car Dynamic Simulator) model. The spring constant of the single equivalent spring representing the combined draft gears of the hammer and anvil railcars has been defined in Reference 1 as:

$$k_T = \frac{k_{RCDG}\, k_{FDG}}{k_{RCDG} + k_{FDG}} \qquad (1)$$

where

k_T = the spring constant of the single equivalent spring representing the combined draft gears of the hammer and anvil rail cars, lbs(force)/inch

k_{RCDG} = the spring constant of the single equivalent spring representing the combined spring and friction damper of the draft gear on the hammer car, lbs(force)/inch

k_{FDG} = the spring constant of the single equivalent spring representing the combined spring and friction damper of the draft gear on the anvil car, lbs(force)/inch

The spring constants k_{RCDG} and k_{FDG} were also defined in Reference 1 by the equations

$$k_{RCDG} = k_1 \left[1 + \mu_D \, \mathrm{sgn}(\dot{X}_T)\right] \qquad (2)$$

and

$$k_{FDG} = k_2 \left[1 + \mu_D \, \mathrm{sgn}(\dot{X}_T)\right] \qquad (3)$$

where

k_1 = the spring constant of the spring in the hammer car draft gear, lbs(force)/inch

k_2 = the spring constant of the spring in the anvil car draft gear, lbs(force)/inch

μ_D = a multiplying factor corresponding to a coefficient of friction for the damper in a draft gear

$\dot{X}_T$ = the total relative velocity of displacement or travel of the two rail cars, inches/sec

and

$sgn(\dot{X}_T)$ = a sign function with $\dot{X}_T$ as the argument [see expression (8) of Reference 1].

Equations (2) and (3) define the equivalent spring constants of the draft gears in their "active" state, i.e., when the total displacement lies between its upper and lower limits. When these limits are reached, the draft gears go "solid", i.e., they behave like a solid beam with properties consistent with the structural characteristics of the draft gears and rail cars. Consequently, the definitions of k_{RCDG} and k_{FDG} were modified to represent the transition from the "active" to the "solid" states. This is accomplished by branching within the model equivalent to the following:

$$\left.\begin{aligned} k_{RCDG} &= k_1 \left[1 + \mu_D \, sgn(\dot{X}_T)\right] \\ k_{FDG} &= k_2 \left[1 + \mu_D \, sgn(\dot{X}_T)\right] \end{aligned}\right\} \qquad X_{TL} < X_T < X_{TU} \qquad (4)$$

and

$$\left.\begin{aligned} k_{RCDG} &= k_{SDG1} \\ k_{FDG} &= k_{SDG2} \end{aligned}\right\} \qquad X_T \leq X_{TL} \text{ or } X_T \geq X_{TU} \qquad (5)$$

where

X_{TL}, X_{TU} = the lower and upper limits, respectively, on the travel of the combined draft gears, inches

k_{SDG1}, k_{SDG2} = the spring constants of the "solid" draft gears on the hammer car and anvil car, respectively, lbs(force)/inch.

Two sets of simulation runs were made during the previous reporting period, using CARDT, for various values of the "solid" draft gear spring constants k_{SDG1} and k_{SDG2}.[2] In one set of runs, the values used ranged from 2.0×10^5 to 1.0×10^6 lbs(force)/inch. The time-varying coupler force following a 6 mile/hour impact between two 70-ton hopper cars loaded with gravel, calculated by the CARDT model, was compared with the coupler force recorded during an actual test, as reported by Baillie.[3] Comparisons made for "solid" state spring constants of 5×10^5 and 1×10^6 lbs(force)/inch are presented as Figures 10 and 11, respectively, in Reference 2.

The second set of simulation runs was based on "solid" draft gear spring constants that were allowed to vary as functions of the relative displacement

$$X_T = X_{RC} - X_F \tag{6}$$

beyond the maximum value of X_T for the "active" state. The spring constants increased in magnitude as X_T increased beyond this "active" limit. The spring constants were expressed as the products of pre-selected base values and a multiplying factor which varied as a function of X_T beyond its active limit, as shown in Equations (7) and (8), and conditions (9).

$$k_{SDG1} = k_{SDG10}\,\phi(X_T) \tag{7}$$

$$k_{SDG2} = k_{SDG20}\,\phi(X_T) \tag{8}$$

where

k_{SDG10}, k_{SDG20} = base spring constants corresponding to k_{SDG1} and k_{SDG2}, respectively, lbs(force)/inch

$\phi(X_T)$ = a multiplying factor where

$$\left.\begin{aligned} \phi(X_T) &= 1.0 \quad \text{when } X_T = 5.6 \text{ inches} \\ \phi(X_T) &> 1.0 \quad \text{when } X_T > 5.6 \text{ inches} \end{aligned}\right\} \tag{9}$$

The lower limit on the base "solid" state spring constants was set at the value of the "active" state spring constant. The lower limit on the multiplying factor was 1.0, and the upper limit was an extrapolation from an arbitrary upper value of 6.35 inches set for X_T. This previous work formed the basis for the development of the car to car characterization function presented here.

The time-varying coupler force calculated using Equations (7) and (8), was compared with Baillie's data in Figure 17 of Reference 2. The calculated coupler force vs time curve had the characteristic shape of the experimental curve, but both its magnitude and duration were substantially larger than those of the experimental curve. It was determined that, if the "solid" draft gear spring constants were bounded at some upper value less than that reached at zero relative velocity (i.e., $dX_T/dt = 0$), the peak coupler force would be reduced, but the duration would be increased. It was further determined that the duration could then be reduced by extracting a suitable fraction of the potential energy stored in the springs. To accomplish these two effects, Equations (7) and (8), and conditions (9), were modified as follows:

$$k_{SDG1} = k_{SDG10}\phi(X_T)[1 + \mu_{XT}\, \mathrm{sgn}(\dot{X}_T)] \tag{10}$$

$$k_{SDG2} = k_{SDG20}\phi(X_T)[1 + \mu_{XT}\ sgn(\dot{X}_T)] \tag{11}$$

and

$$\left.\begin{aligned} \phi(X_T) &= \phi(X_T)_L \quad \text{when } X_T \leq 5.6 \text{ inches} \\ \phi(X_T) &= \phi(X_T) \quad \text{when } 5.6 < X_T < 6.35 \text{ inches} \\ \phi(X_T) &= \phi(X_T)_U \quad \text{when } X_T \geq 6.35 \text{ inches} \end{aligned}\right\} \tag{12}$$

where

μ_{XT} = a multiplying factor representing the extent of energy dissipation ($0 \leq \mu_{XT} \leq 1$).

When the draft gears bottom out and enter their "solid" state, the relative displacement X_T no longer represents the travel of the combined draft gears. The terms X_{RC} and X_F are the horizontal displacements of the centers of gravity (cg) of the hammer car and anvil car, respectively. During the "solid" state of the draft gears, the cargo shifts or displaces causing a shift or change in these displacements even though the actual travel of the draft gears during this period may be very slight. Consequently, the coupler force between the cars becomes a function of the resistance of the cargo to shift or deformation. A load-deflection curve for the cargo during this period would be based on cargo displacement relative to that of the rail car (i.e., displacement of the cg), and would produce a pseudo spring constant with the characteristics of the "solid" draft gear spring constants described in the previous paragraph. It is assumed that no cargo shifting or deformation occurs during the "active" state of the draft gears. This pseudo spring constant or "solid" draft gear spring constant also contains a term which accounts for the dissipation of a large portion of the energy required to shift or deform the cargo. Normally, a spring would restore to the system its energy of compression. In cargo shifting and deformation, energy is dissipated due to friction and due to permanent deformation of the cargo. Therefore, in the model, when the cargo is no longer compelled to move in the direction of greater compaction, the energy stored in the spring

is discarded from the system by a substantial reduction in the spring constant for the recovery phase. This is accomplished by adjusting the parameter μ_{XT}. During compaction or shifting of the cargo, when the relative velocity $\dot{X}_T$ is positive, μ_{XT} is set at 0 or some small fraction. At the end of compaction when the spring would normally restore the energy of compaction to the system and when $\dot{X}_T$ is negative, μ_{XT} is set at some large fraction. μ_{XT} is defined by

$$\left.\begin{aligned} \mu_{XT} &= \mu_{XTC} \qquad \text{when } \dot{X}_T > 0 \text{ (Compaction)} \\ \mu_{XT} &= \mu_{XTE} \qquad \text{when } \dot{X}_T \leq 0 \text{ (Recovery)} \end{aligned}\right\} \tag{13}$$

where

μ_{XTC} = an energy dissipation coefficient for cargo compaction

μ_{XTE} = an energy dissipation coefficient for the cargo recovery phase.

The equivalent spring constants of the draft gears in both their "active" and "solid" states may be summarized by restating Equation (4) and combining Equations (5), (10) and (11) to give

$$\left.\begin{aligned} k_{RCDG} &= k_1 \left[1 + \mu_D \operatorname{sgn}(\dot{X}_T)\right] \\ k_{FDG} &= k_2 \left[1 + \mu_D \operatorname{sgn}(\dot{X}_T)\right] \end{aligned}\right\} \qquad X_{TL} < X_T < X_{TU} \tag{4}$$

for the "active" state, and

$$\left.\begin{aligned} k_{RCDG} &= k_{SDG10}\phi(X_T) \left[1 + \mu_{XT}\operatorname{sgn}(\dot{X}_T)\right] \\ k_{FDG} &= k_{SDG20}\phi(X_T) \left[1 + \mu_{XT}\operatorname{sgn}(\dot{X}_T)\right] \end{aligned}\right\} \qquad X_T \leq X_{TL} \text{ or } X_T \geq X_{TU} \tag{14}$$

for the "solid" state.

Using the above expressions for the spring constants of the draft gears in the CARDT model, additional runs were made to simulate the 6-mile/hour impact between the two gravel-loaded 70-ton hopper cars discussed earlier. During these runs, values of the parameters k_{SDG10}, k_{SDG20}, $\phi(X_T)$, μ_{XTC} and μ_{XTE} were adjusted to obtain a coupler force vs time curve that compared reasonably well with the actual data reported by Baillie[3] for this experiment. Final values of these and other pertinent parameters are summarized in Table 1. The parameter $\phi(X_T)$ is presented in Figure 1. Results of the latest simulation runs are compared with experimental results in Figures 2 through 5. Coupler forces, relative displacements of the centers of gravity of the cars, relative velocities and relative accelerations are compared in Figures 2, 3, 4 and 5, respectively. Good comparisons were obtained up to about 0.076 second after impact. Beyond this time the response variables deviate as shown, indicating that further adjustments in the parameters are required. The experimental coupler force peaks at about 0.07 second while the calculated force peaks at about 0.085 second. The calculated coupler force as a function of calculated relative displacement is presented in Figure 6. This load-deflection curve for the single equivalent spring separating the rail cars encompasses both the "active" and "solid" states of the draft gears. The shape of the cyclic curve of Figure 6 is not unlike the curves presented by Kasbekar[4] and Scales[5] for standard draft gears.

The "goodness" of the comparisons of the calculated and experimental coupler forces, relative displacements, relative velocities and relative accelerations has been expressed in terms of Theil's inequality coefficients for each response variable and Theil's multiple inequality coefficient for the simultaneous comparison of all the response variables (see Section 3. VALIDATE MODEL).

The CARDS model was modified to include equations equivalent to Equations (4), (13) and (14), and the function presented in Figure 1. Sets of equations were written to represent the linkage between the cask-rail car (hammer car) and the first coal-filled anvil car, and the linkages between the remaining three coal-filled anvil cars. However, an additional control

TABLE 1

PARAMETERS USED IN THE *CARDT* MODEL FOR SIMULATION OF IMPACT BETWEEN TWO HOPPER CARS LOADED WITH GRAVEL

Weight of the Hammer Car, lbs(force) W_{RC}	218,000
Weight of the Anvil Car, lbs(force) W_F	211,000
Upper Limit on Travel of Combined Draft Gears, inches X_{TU}	5.6
Lower Limit on Travel of Combined Draft Gears, inches X_{TL}	-5.6
Spring Constants of Draft Gears During the "Active" State, lbs(force)/inch k_1, k_2	48,666
Base Spring Constants of Draft Gears During the "Solid" State, lbs(force)/inch k_{SDG10}, k_{SDG20}	75,000
Energy Dissipation Coefficient for Cargo Compaction Phase μ_{XTC}	0.01
Energy Dissipation Coefficient for Cargo Recovery Phase μ_{XTE}	0.9

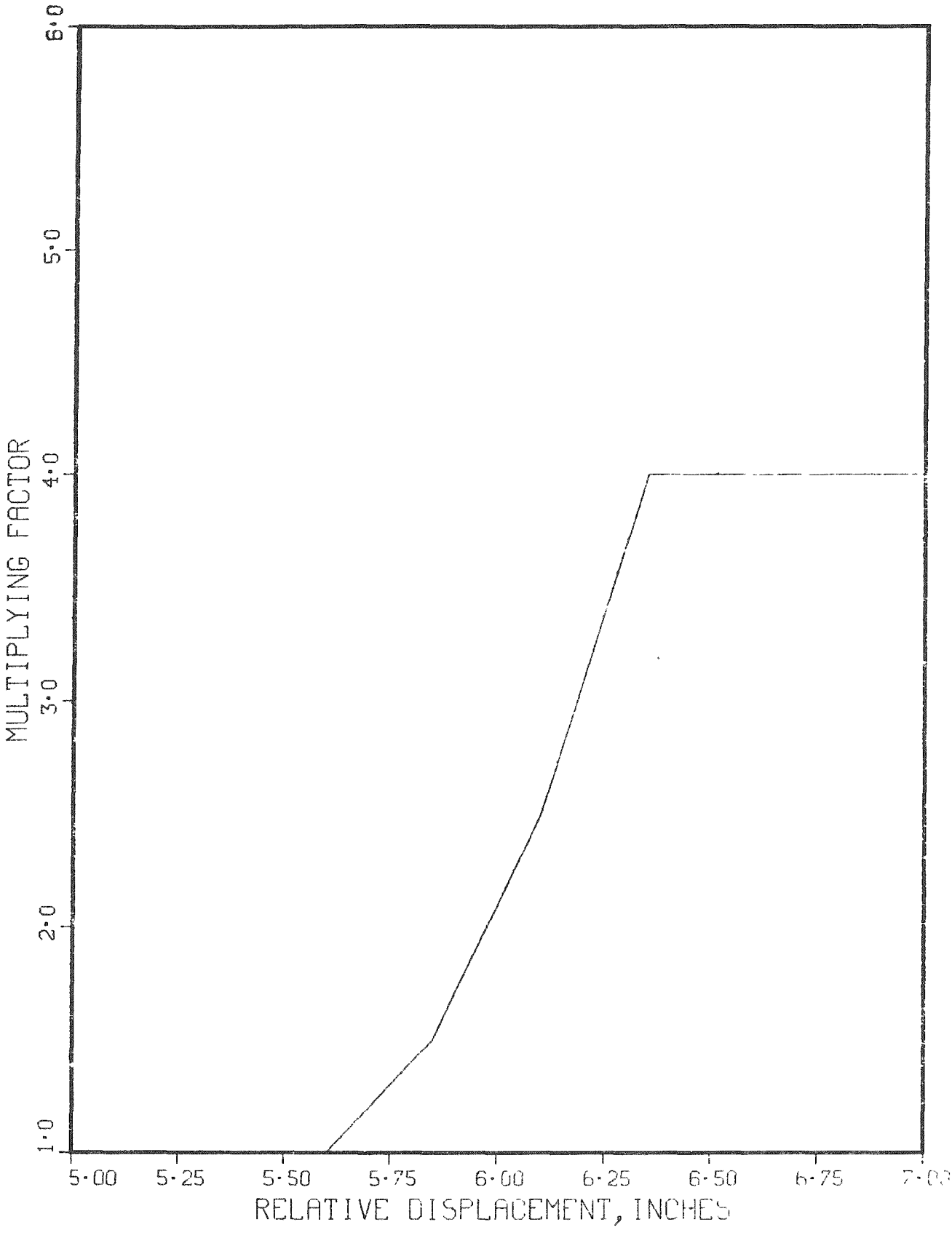

FIGURE 1. Ratio of "Solid" Draft Gear Spring Constant to a Base Value.

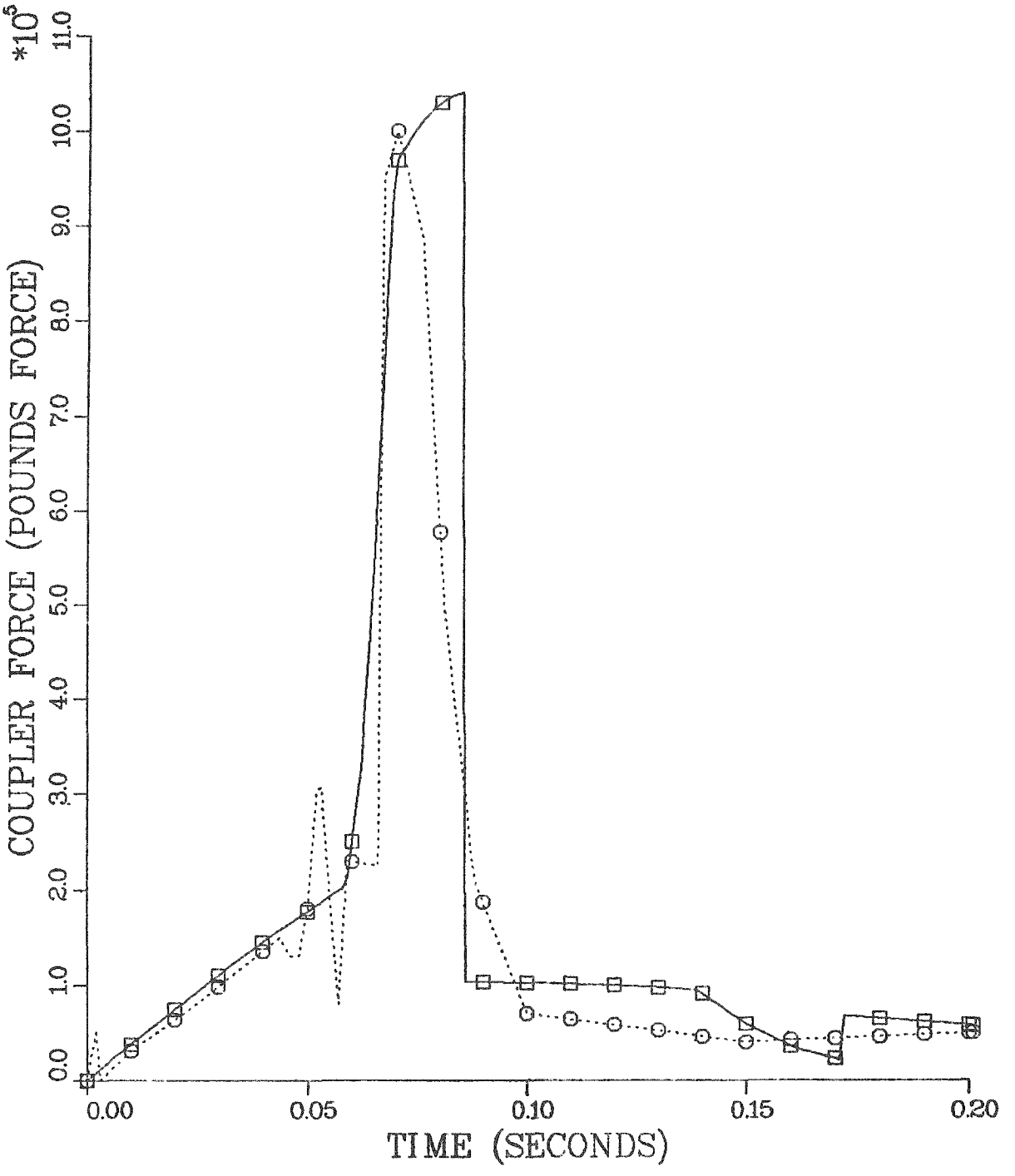

FIGURE 2. Coupler Force vs Time During Impact of Two Hopper Cars Loaded With Gravel.

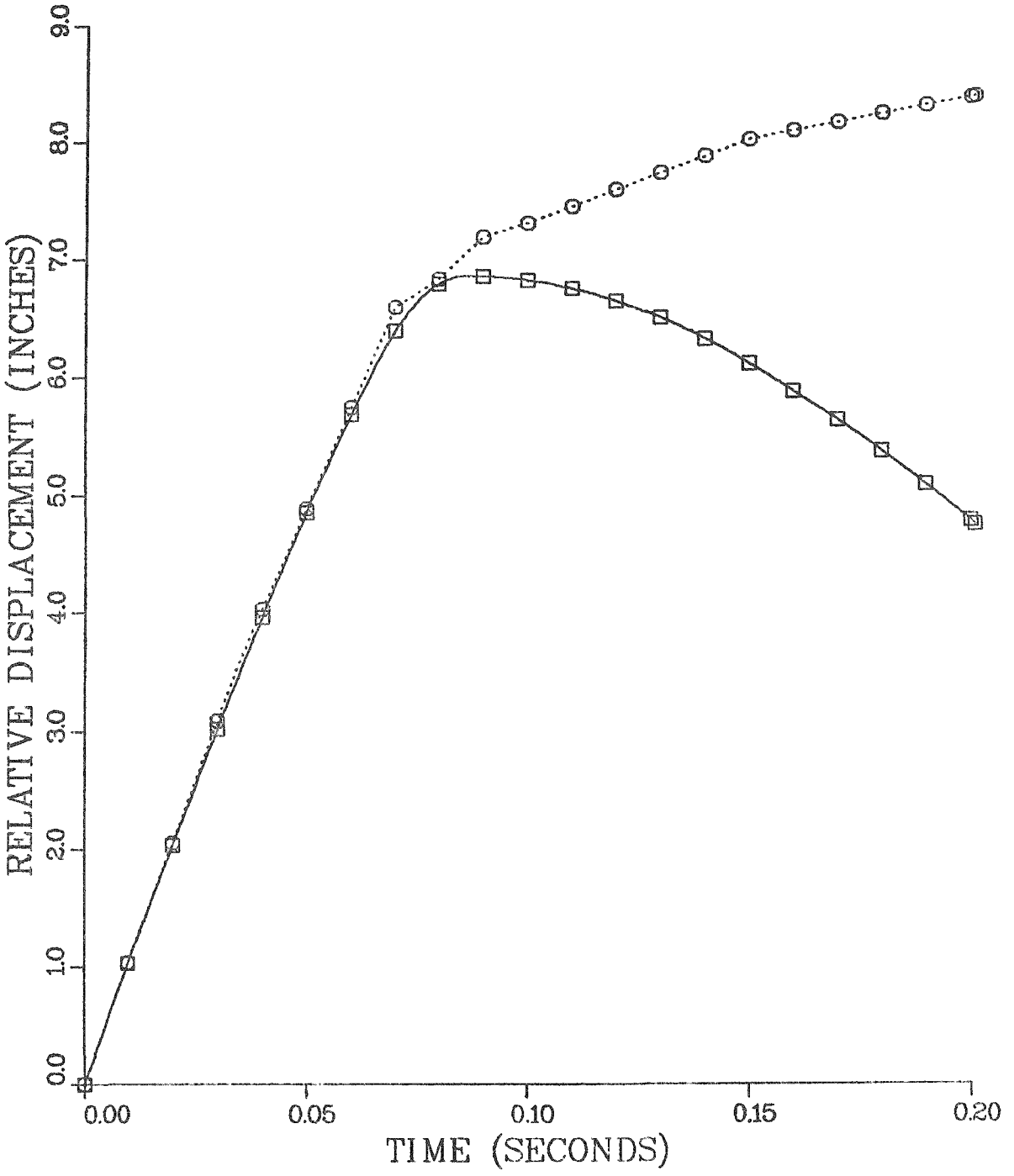

FIGURE 3. Relative Displacement of Two Gravel-Filled Hopper Cars vs Time During Impact.

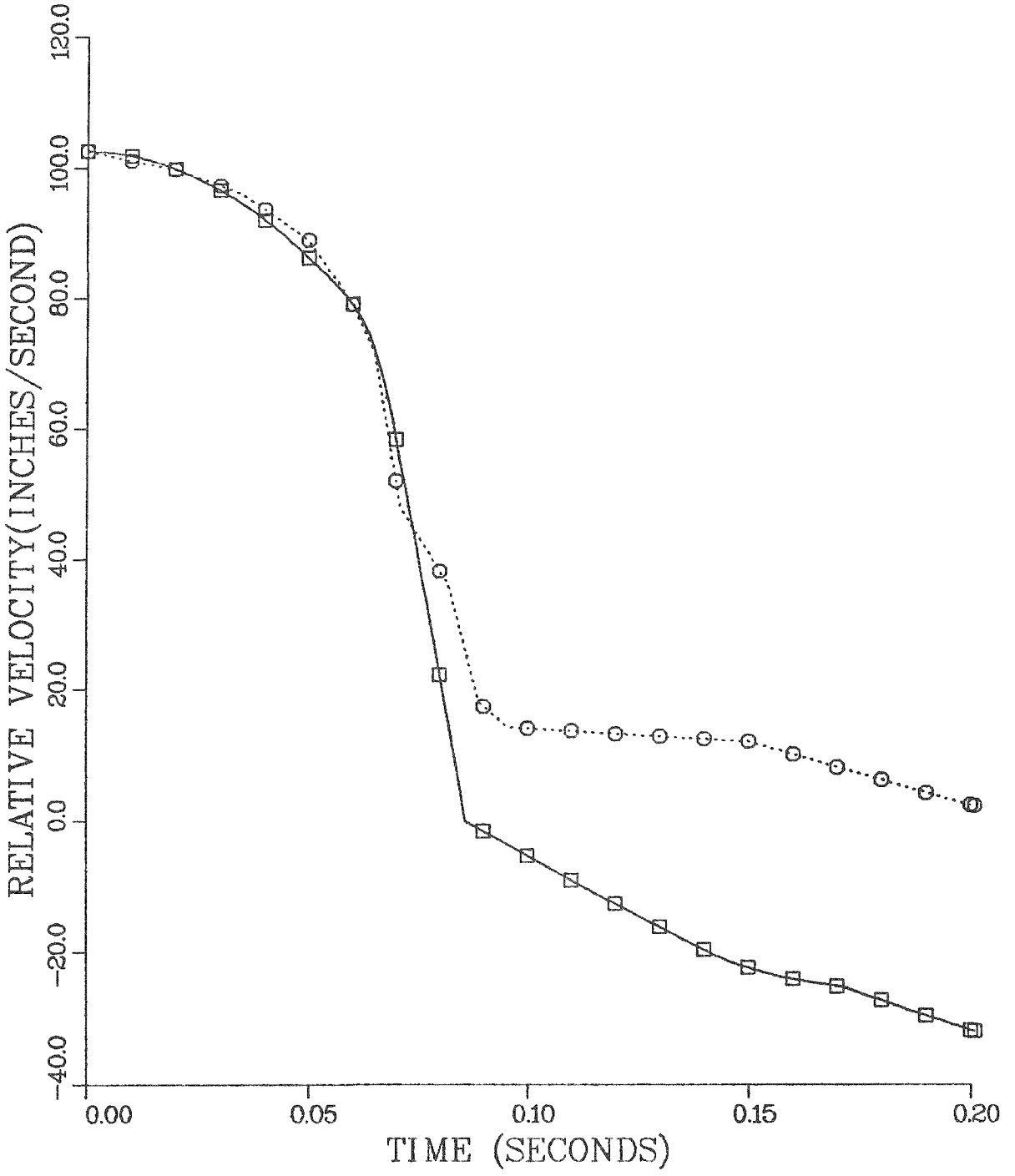

FIGURE 4. Relative Velocity of Two Gravel-Filled Hopper Cars vs Time During Impact.

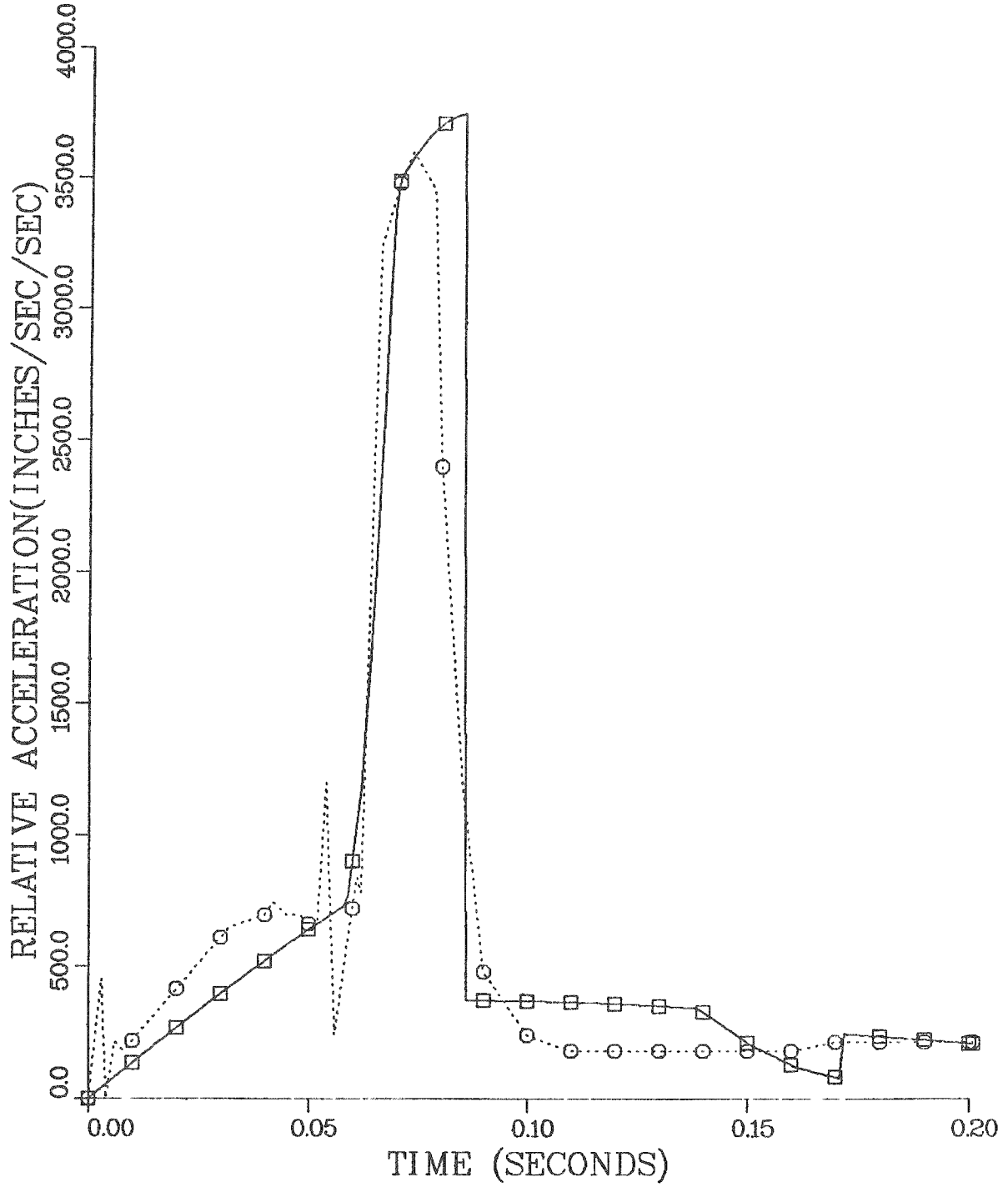

FIGURE 5. Relative Acceleration of Two Gravel-Filled Hopper Cars vs Time During Impact.

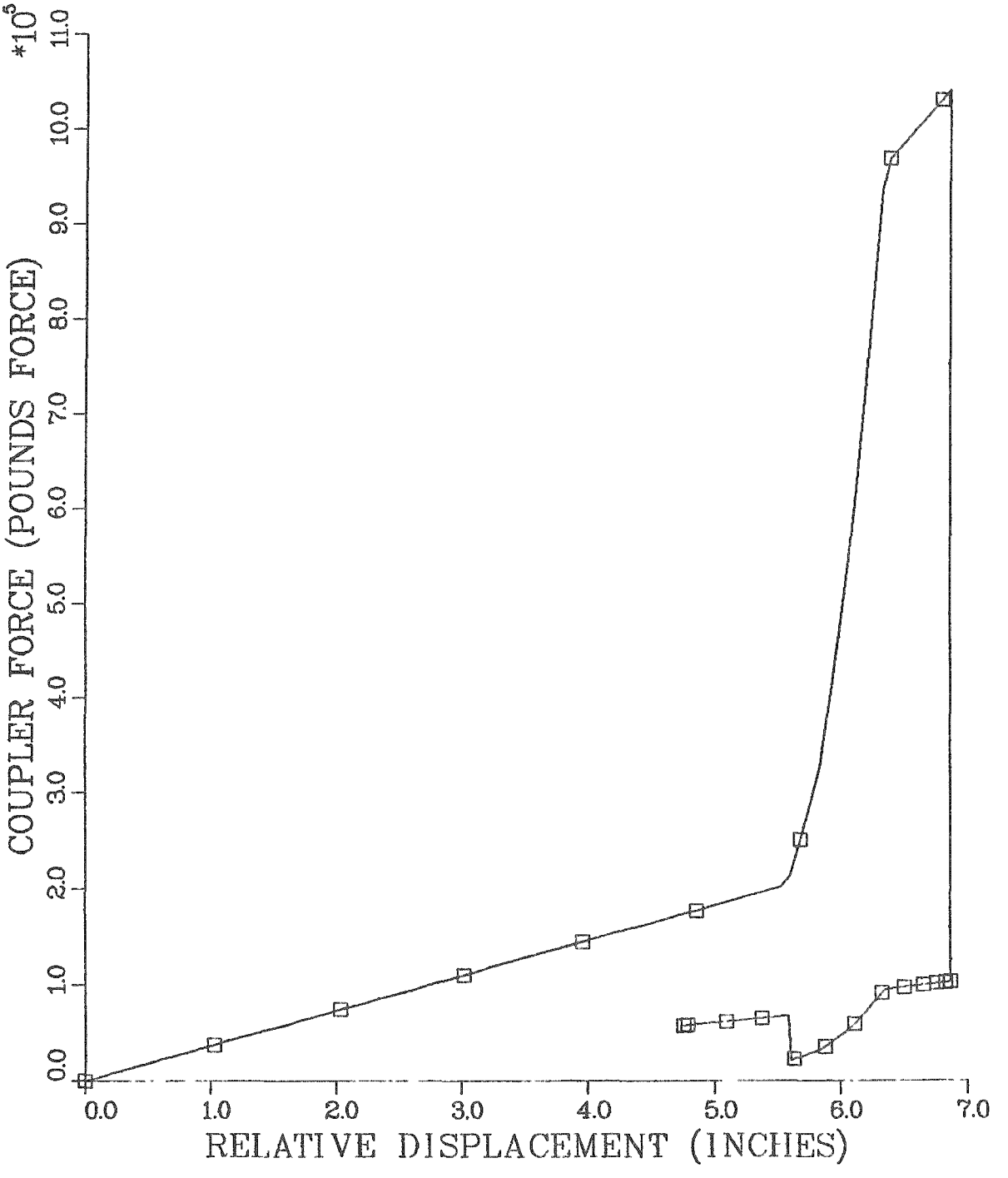

FIGURE 6. Calculated Coupler Force vs Calculated Relative Displacement of Two Gravel-Filled Hopper Cars During Impact.

variable was required since the cargo of the cask-rail car (the cask) is considered as a separate mass with its own equation of motion. Also, the trucks on the rail car are considered as separate masses with their own equations of motion. Consequently, since the character of the cask-rail car is known and modeled accordingly, that portion of the car characterization function for the hammer car-anvil car linkage need not include the effects of cargo compaction and energy dissipation. To accomplish this, the control variable RCOR was introduced to provide control over the draft gear spring constant during the "solid" state. RCOR was added as a restriction on Equation set (14) as follows:

$$\begin{aligned} k_{RCDG} &= k_{SDG10}\phi(X_T)[1 + \mu_{XT}\ \mathrm{sgn}(\dot{X}_T)] \quad X_T \leq X_{TL} \text{ or } X_T \geq X_{TU} \\ &\qquad\qquad\qquad\qquad\qquad\qquad\qquad\qquad\qquad\qquad \text{and} \\ k_{FDG} &= k_{SDG20}\phi(X_T)[1 + \mu_{XT}\ \mathrm{sgn}(\dot{X}_T)] \quad RCOR = 0 \end{aligned} \tag{14}$$

$$\begin{aligned} k_{RCDG} &= k_{SDG10} \quad X_T \leq X_{TL} \text{ or } X_T \geq X_{TU} \\ &\qquad\qquad\qquad\qquad\qquad\qquad\qquad\qquad\qquad\qquad \text{and} \\ k_{FDG} &= k_{SDG20}\phi(X_T)[1 + \mu_{XT}\ \mathrm{sgn}(\dot{X}_T)] \quad RCOR = 1. \end{aligned} \tag{15}$$

where

RCOR = cask-rail car override variable, with the control function:

RCOR = 1.0, to override railcar characterization function

RCOR = 0., to activate railcar characterization function

After the above modifications to the CARDS model were completed, preliminary runs were made to compare the calculated coupler force with that measured during Test 3 of the cask-rail car humping tests conducted at the Savannah River Laboratories in July and August of 1978. The latest calculated coupler force is compared with experimental data in Figure 7. The conditions of Test 3 are summarized in Table 2 of Reference 1. During these

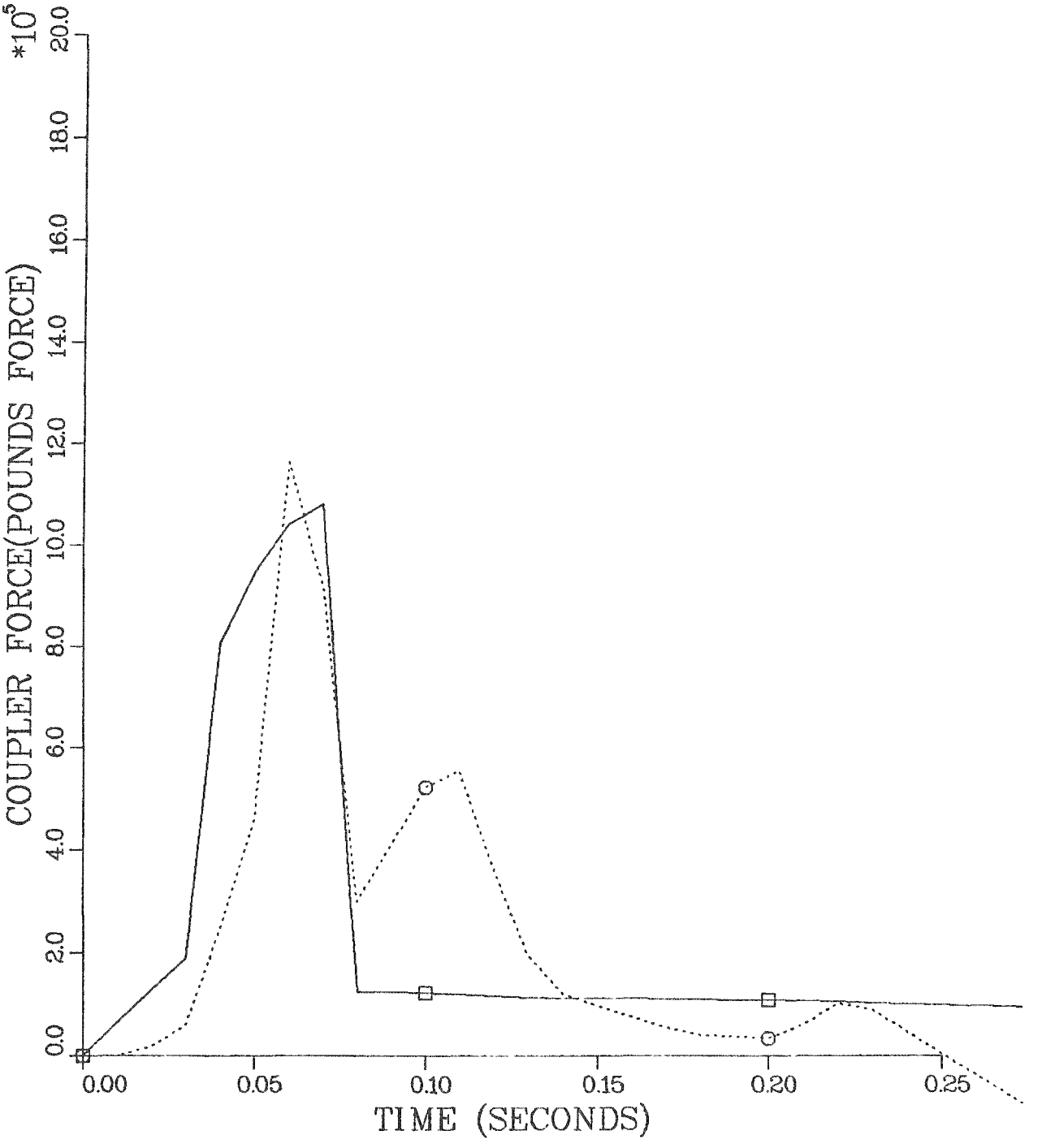

FIGURE 7. Coupler Force vs Time During Impact of Cask-Rail Car with Four Hopper Cars Loaded with Coal.

runs, the parameters k_{SDG20}, $\phi(X_T)$, μ_{XTC} and μ_{XTE} were held at the values listed in Table 1. However, the parameter k_{SDG10} was increased to 200,000 lbs(force)/inch.

Initial comparison of the time-varying calculated and experimental coupler forces showed that the ramps and peaks of the experimental curve lagged considerably behind those of the calculated curve. Since the starting time for the CARDS simulation is the time at which the coupler begins to travel, this suggested that perhaps the recording device installed for the experiment was activated by almost imperceptible movements of the coupler mechanism prior to significant compression. Frame by frame examination of the high speed film of this portion of Test 3 showed that, from the instant of initial contact between the couplers to the first sign of draft gear travel, 9 frames were exposed. At 400 frames per second, this meant that 0.0225 second had elapsed over this interval. A shift of the results by this amount of time produced much better agreement between the times at which the various events occurred (see Figure 7).

The calculated horizontal force exerted on the hammer rail car by the cask (i.e., the "longitudinal" or horizontal restraint force) is compared with the "longitudinal" force measured during the test in Figure 8. The same time shift used for the coupler force in Figure 7 was used for the results in Figure 8.

Both the measured forces of Figures 7 and 8 peak twice within 0.2 second of the transient. Corresponding forces calculated using the CARDS model peak only once during this period, but the pulses agree reasonably well with the first peaks of the experimental curves. Further modification of the characterization function is required to duplicate the secondary peaks in the experimental curves.

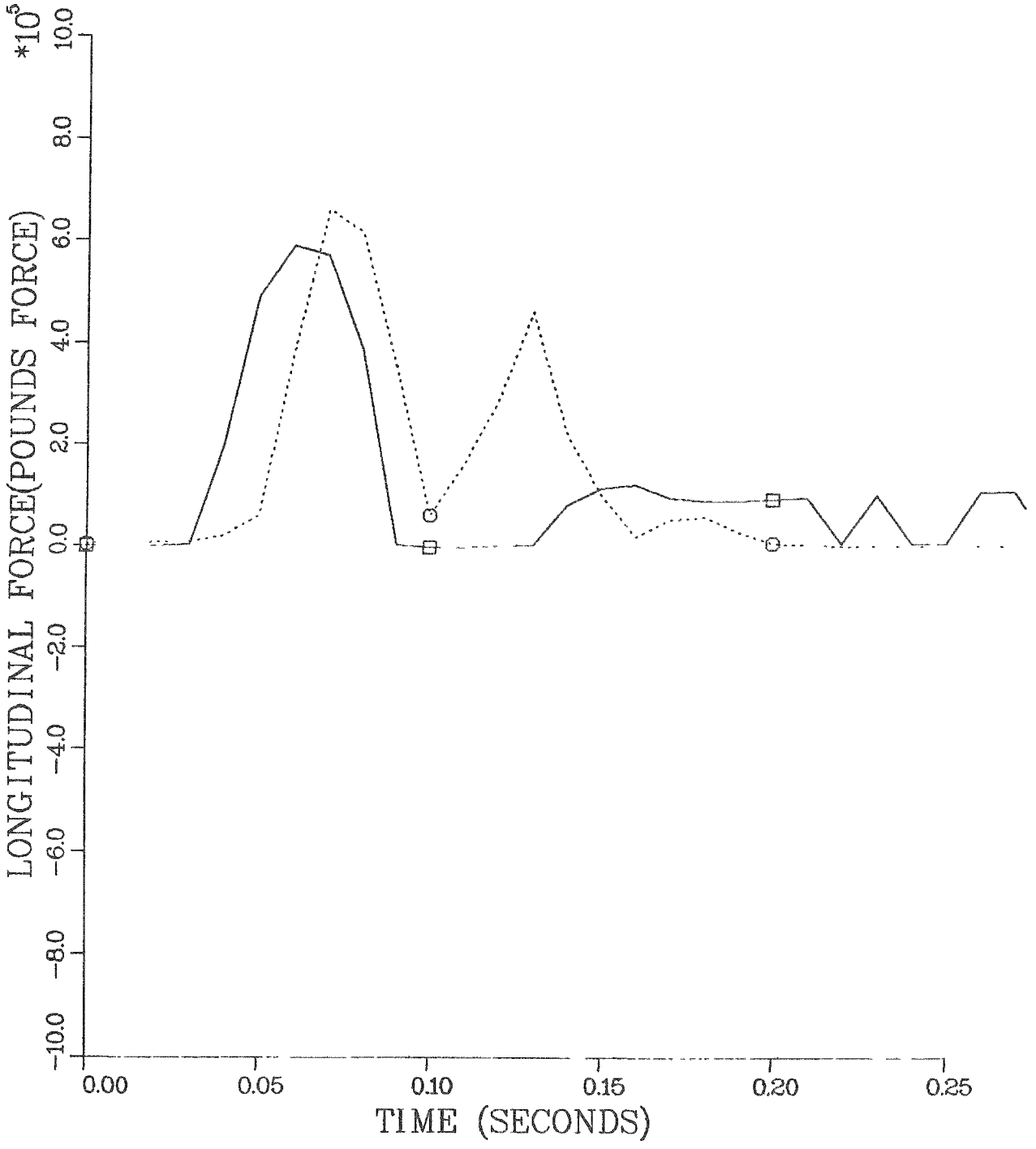

FIGURE 8. Horizontal Force of Interaction Between Cask and Rail Car vs Time During Impact with Four Hopper Cars Loaded with Coal.

2. DATA COLLECTION AND REDUCTION

Recent efforts to read the reduced experimental data into the Boeing Computer Sciences (BCS) Univac computer system have been successful. This allows access to both the experimental and corresponding calculated data files for comparison using two coupled post-processing programs for model validation (see Section 3. VALIDATE MODEL).

Problems of data alignment, necessary for comparison and model validation, have been anticipated and initial solutions conceived. One such problem is that the initiation of experimental data collection is keyed to the slightest initiation of displacement of the instrumented coupler which precedes the actual compression of the draft gears, whereas immediate compression of the draft gears is assumed as the starting point in the calculation of data using the analytical models. The difference between the two is a time delay which can be measured by cross-correlation or, in some cases, by inspection and measurement of the two corresponding parameters in the experimental data (see Section 1. DEVELOP DYNAMIC MODEL). In a similar manner, the frequency domain parameters can be aligned if the frequency axis is converted from a scale linear in frequency to the log of the frequency.

Efforts to recover data on Tests 1, 2 and 3, whose timing tracks were lost during transcription, have not been successful. Sandia Laboratories has replaced these data with copies of their data on BCS compatible tape.

3. VALIDATE MODEL

A measure of how well the CARDT model simulates the behavior of an actual hammer car-anvil car system was obtained by quantitatively comparing the calculated coupler forces, relative displacements of the centers of gravity of the cars, the relative velocities, and the relative accelerations with those recorded during a 6-mile/hour impact between two 70-ton hopper cars loaded with gravel.[3] Visual comparisons are presented in Figures 2 through 5 (see Section 1. DEVELOP DYNAMIC MODEL). Quantitative comparisons

were made using Theil's inequality coefficients for each of the response variables listed, and Theil's multiple inequality coefficient for the simultaneous comparison of all the response variables. Theil's inequality coefficient for a single response variable (TIC) has been defined and discussed in Reference 2.

Theil's multiple or overall inequality coefficient (TMIC) is a figure of merit based on the number of observations or data points, the values of several output or response variables selected at discrete points, and the two-variable inequality coefficients (TICs) defined by Equation (5) in Reference 2. The two-variable (calculated and experimental variable values) inequality coefficients are combined to generate the TMIC.[6] The TMIC is defined by

$$TMIC = \frac{(PPD+PXD)TICD+(PPV+PXV)TICV+(PPA+PXA)TICA+(PPF+PXF)TIC}{2(PPD+PXD+PPV+PXV+PPA+PXA+PPF+PXF)} \tag{16}$$

where

$$PPD = \sqrt{\frac{X_T^2}{n}} \tag{17}$$

$$PXD = \sqrt{\frac{X_{TX}^2}{n}} \tag{18}$$

$$PPV = \sqrt{\frac{\dot{X}_T^2}{n}} \tag{19}$$

$$PXV = \sqrt{\frac{\dot{X}_{TX}^2}{n}} \tag{20}$$

$$PPA = \sqrt{\frac{\ddot{X}_T^2}{n}} \tag{21}$$

$$PXA = \sqrt{\frac{\ddot{X}_{TX}^2}{n}} \tag{22}$$

$$PPF = \sqrt{\frac{F_{CPL}^2}{n}} \tag{23}$$

$$PXF = \sqrt{\frac{F_{CPLX}^2}{n}} \tag{24}$$

The terms in these equations are

TMIC = Theil's multiple inequality coefficient

TIC,TICD,TICV,TICA = Theil's two-variable inequality coefficients for comparison of calculated and experimental values of coupler force, relative displacement, relative velocity, and relative acceleration, respectively.

F_{CPL}, F_{CPLX} = calculated and experimental coupler forces, respectively, lbs(force)

X_T, X_{TX} = calculated and experimental relative displacements, respectively, inches

$\dot{X}_T, \dot{X}_{TX}$ = calculated and experimental relative velocities respectively, inches/second

$\ddot{X}_T, \ddot{X}_{TX}$ = calculated and experimental relative accelerations, respectively, inches/sec/sec

n = number of observations or sampling points

Equations (16) through (24) were added to the CARDT model for calculation of the TMIC during the simulation discussed in Section 1. The values of TMIC from Equation (16) will vary between the following two extremes:

TMIC = 0 (the case of equality or perfect agreement)
TMIC = 1 (the case of maximum inequality or poor agreement)

Theil's inequality coefficients for the response variables of Figures 2, 3, 4 and 5 are presented as Figures 9, 10, 11 and 12, respectively. Theil's multiple inequality coefficient is presented in Figure 13. The final value of the multiple coefficient of Figure 13 is about 0.106 which indicates that the model accomplishes a reasonably good simulation of the experiment. However, it is also an indication that further refinements and adjustments are necessary to drive TMIC as close to 0 as possible.

Three post-processing programs have been developed to process both the output from simulation runs using CARDT and CARDS, and reduced experimental data. The first of these is the computer program FFT (Fast Fourier Transform), developed as part of the data collection and reduction task to map response variables from the time domain into the frequency domain.[7] The second post-processor program developed is TIC (Theil's Inequality Coefficient) which computes both the two-variable (TIC) and the multiple (TMIC) Theil's inequality coefficients. The FFT and TIC programs have been coupled, as shown in Figure 14, to produce inequality coefficients for the evaluation of model performance based on the comparison of response variables in both the time and frequency domains. Finally, the third post-processing program developed is a plotting routine which produces the plots presented in this

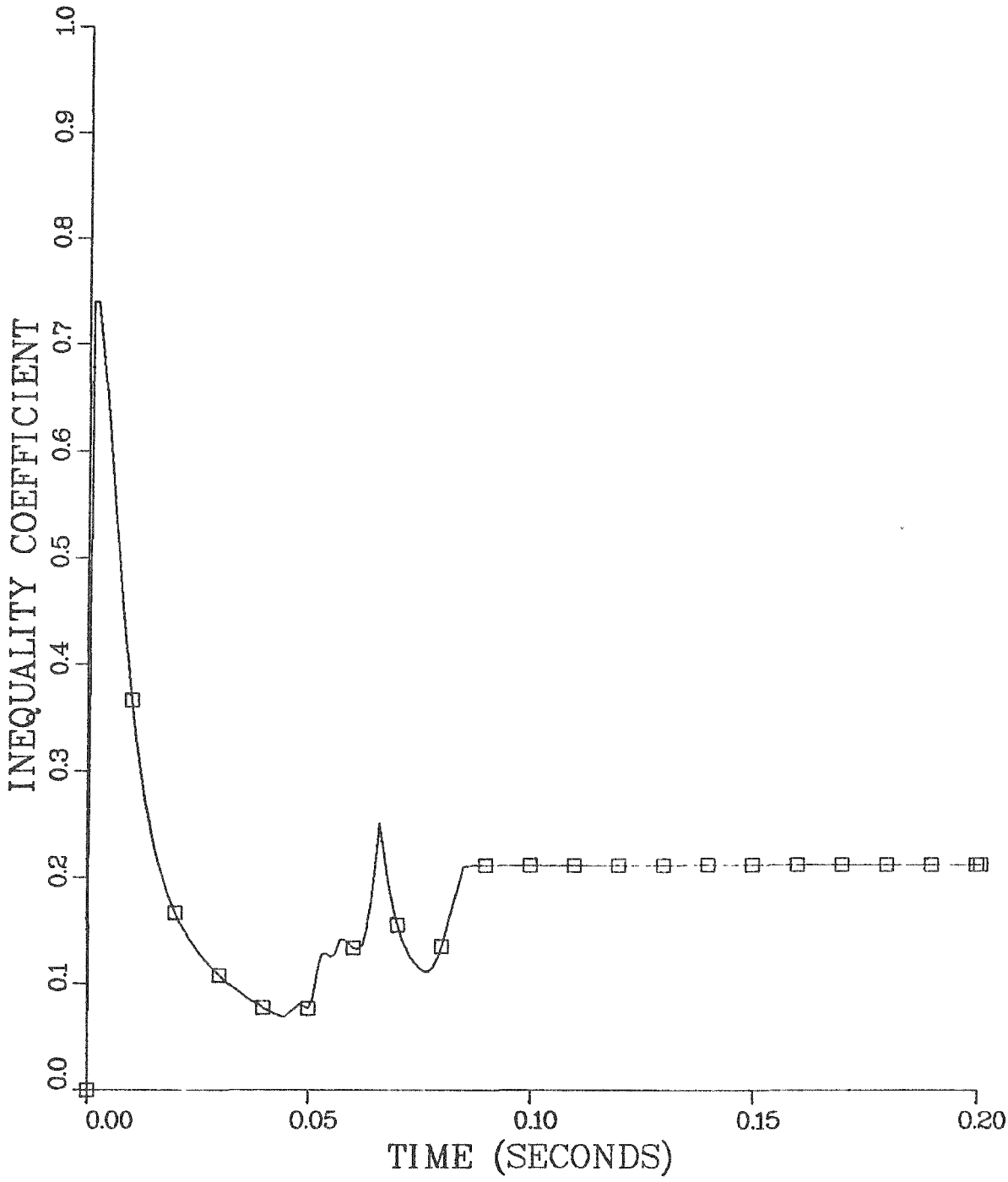

FIGURE 9. Comparison of Calculated and Measured Coupler Forces Using Theil's Inequality Coefficient as a Figure of Merit.

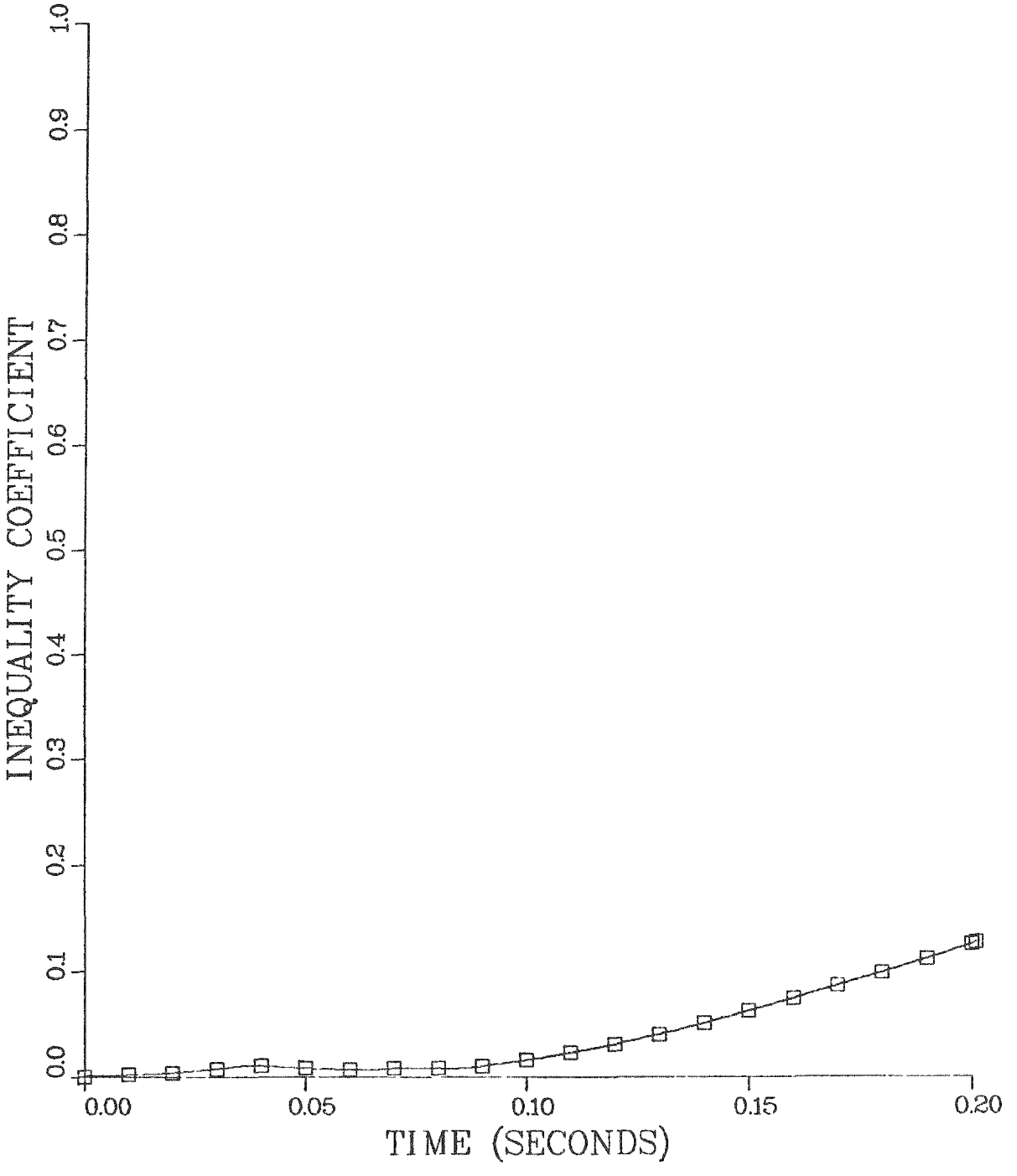

FIGURE 10. Comparison of Calculated and Measured Relative Displacements of Rail Car Centers of Gravity Using Theil's Inequality Coefficient as a Figure of Merit.

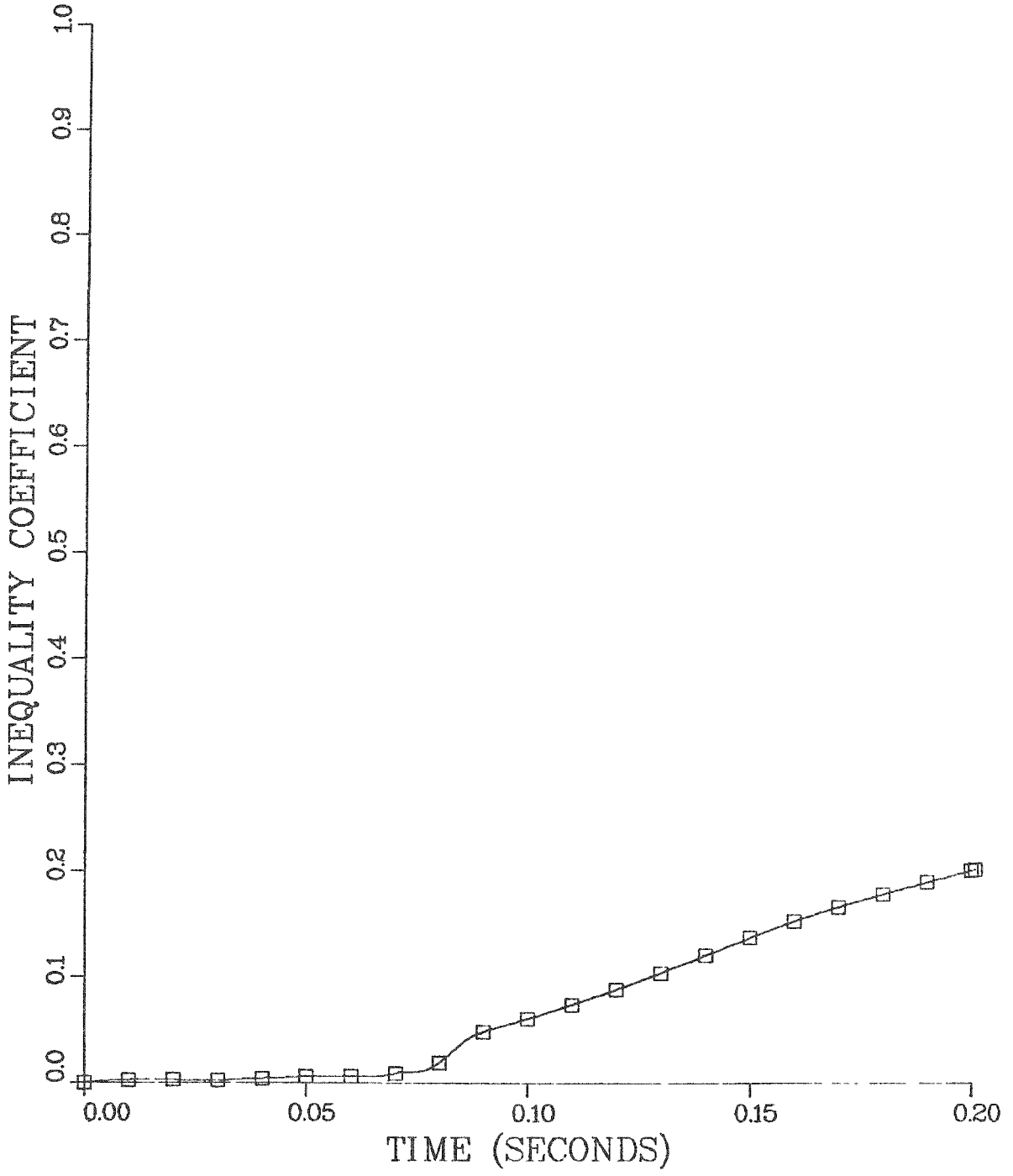

FIGURE 11. Comparison of Calculated and Measured Relative Velocities Using Theil's Inequality Coefficient as a Figure of Merit.

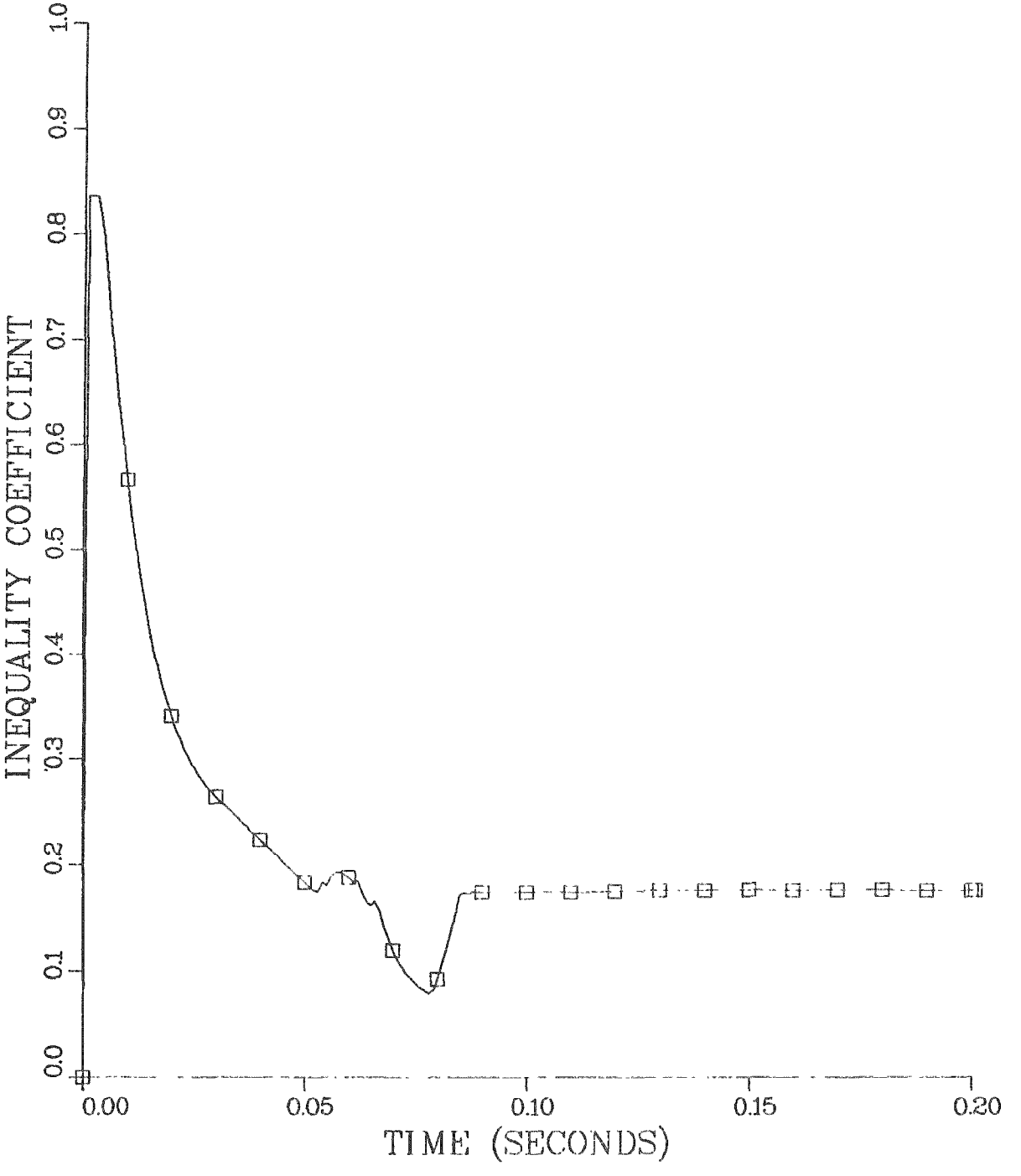

FIGURE 12. Comparison of Calculated and Measured Relative Accelerations Using Theil's Inequality Coefficient as a Figure of Merit.

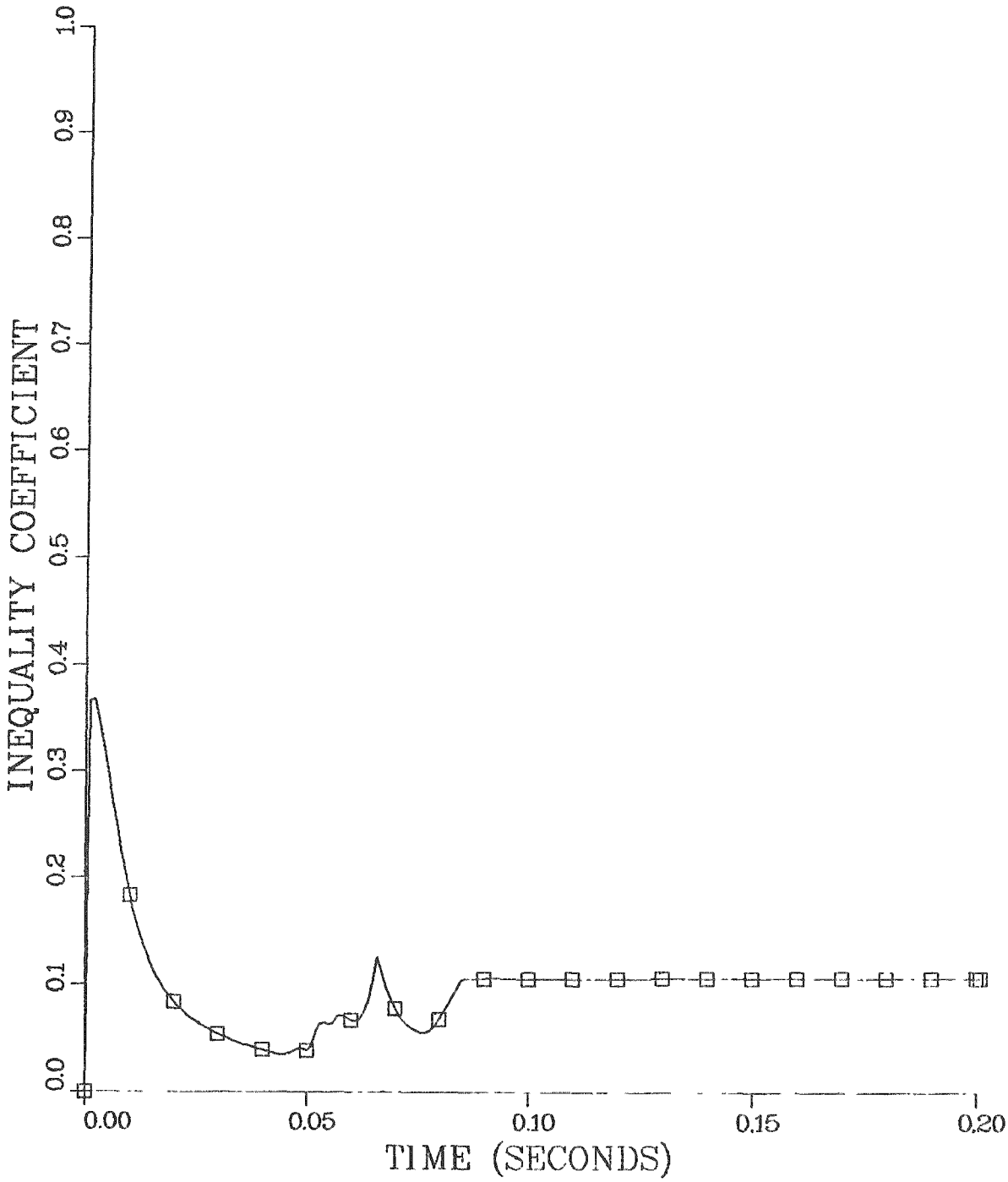

FIGURE 13. Simultaneous Comparison of Calculated and Measured Response Variables Using Theil's Multiple Inequality Coefficient as an Overall Figure of Merit.

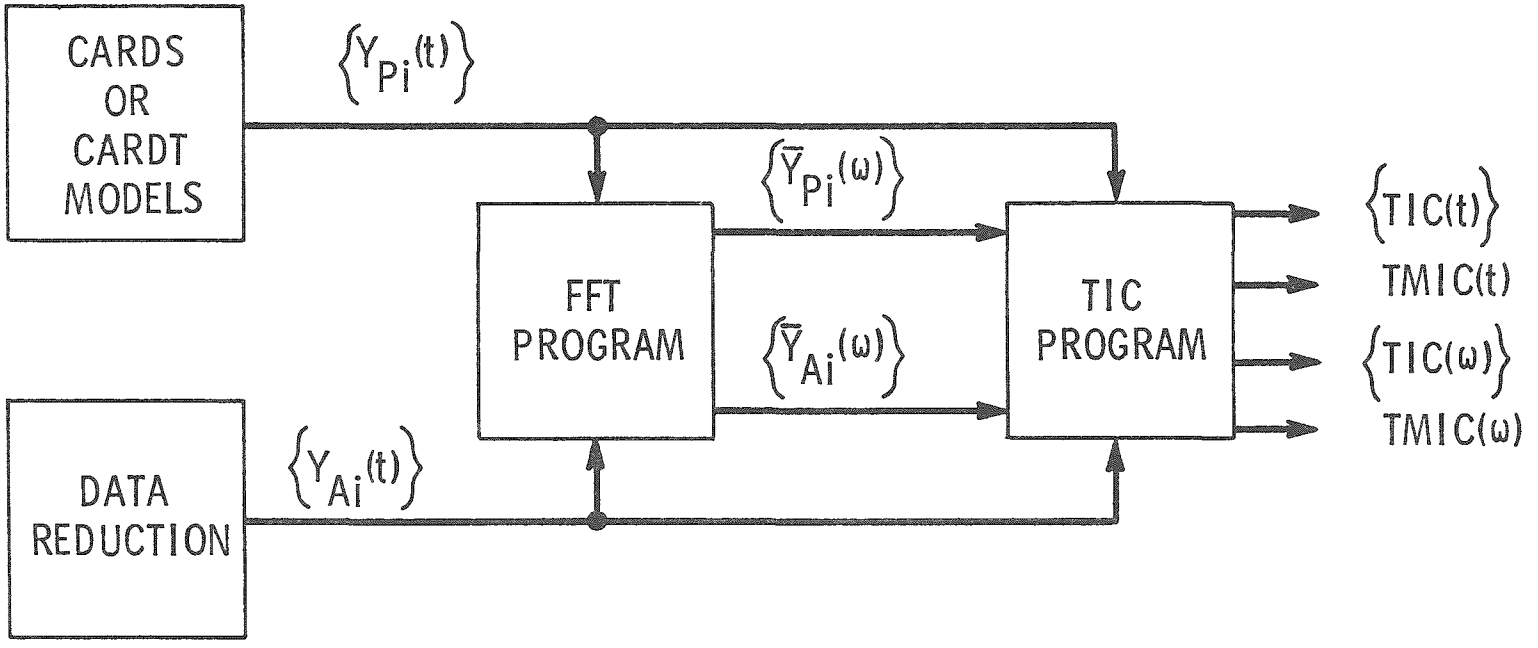

FIGURE 14. Post-Processing Programs for Evaluation of Model Performance by Comparison of Response Variables in Both the Time and Frequency Domains.

series of Quarterly reports. This plotting program provides much greater flexibility in the type and format of plots over those produced by the ACSL language.

In the model performance evaluation process depicted in Figure 14, a set of i predicted time-varying response variables $\{Y_{Pi}(t)\}$ from a simulation model and a corresponding set of actual measured response variables $\{Y_{Ai}(t)\}$ from data reduction are processed by the TIC program to produce a set of Theil's inequality coefficients $\{TIC(t)\}$, one for each of the time-varying response variables. The individual time domain TICs are then used to produce a multiple Theil's inequality coefficient for the time domain, TMIC(t). The $\{Y_{pi}(t)\}$ and $\{Y_{Ai}(t)\}$ are mapped into the frequency domain by the FFT program to produce the equivalent sets $\{\bar{Y}_{Pi}(\omega)\}$ and $\{\bar{Y}_{Ai}(\omega)\}$. The "frequency-varying" sets are then processed by the TIC program to produce a set of frequency-based inequality coefficients, $\{TIC(\omega)\}$, and a frequency-based multiple inequality coefficient, $TMIC(\omega)$.

4. COLLECT PARAMETER DATA

There has been no activity in this task during this reporting period.

5. PARAMETRIC AND SENSITIVITY ANALYSIS

Progress in this task has been closely linked with that reported for Task 1 (DEVELOP DYNAMIC MODEL) and Task 3 (VALIDATE MODEL). The adjustment of parameters to arrive at valid car characterization functions is an important part of this task.

6. INTERIM REPORT

No interim reports were produced during this reporting period.

REFERENCES

1. S. R. Fields and S. J. Mech, Dynamic Analysis to Establish Normal Shock and Vibration of Radioactive Material Shipping Packages, NUREG/CR-0589 (HEDL-TME 78-102), Quarterly Progress Report (July 1, 1978 - September 30, 1978), November 1978.

2. S. R. Fields and S. J. Mech, Dynamic Analysis to Establish Normal Shock and Vibration and Radioactive Material Shipping Packages, NUREG/CR-0880 (HEDL-TME 79-29), Quarterly Progress Report (January 1, 1979 - March 31, 1979), August 1979.

3. W. E. Baillie, "Impact as Related to Freight Car and Loading Damage," ASME Paper 59-A-249, 1959.

4. P. V. Kasbekar, V. K. Garg and G. C. Martin, "Dynamic Simulation of Freight Car and Lading During Impact," Journal of Engineering for Industry, Transactions of the ASME, November 1977.

5. B. T. Scales, "Longitudinal-Shock Problems in Freight Train Operation", ASME Paper 64-WA/RR-4, 1964.

6. N. A. Kheir and W. M. Holmes, "On Validating Simulation Models of Missile Systems", Simulation, April 1978.

7. S. R. Fields and S. J. Mech, Dynamic Analysis to Establish Normal Shock and Vibration of Radioactive Material Shipping Packages, NUREG/CR-0766 (HEDL-TME 79-3), Quarterly Progress Report (October 1, 1978 - December 31, 1979), July 1979.

DISTRIBUTION

RT (195)

DOE/Richland Operations (5)
P.O. Box 550
Richland, WA 99352

Chief Patent Attorney
B. J. Melton
J. D. White (3)

DOE/FFTF Project Office
P.O. Box 550
Richland, WA 99352

Director

DOE/Chicago Patent Office
9800 S. Cass Avenue
Argonne, IL 60439

A. A. Churm

DOE/Environmental Control & Technology Division
Washington, DC 20545

J. Counts

E. I. Dupont de Nemours and Company
P.O. Box A
Aiken, SC 29801

S. F. Petry

Los Alamos Scientific Laboratory
P.O. Box 1663
Los Alamos, NM 87545

T. D. Butler

Pacific Northwest Laboratory
P.O. Box 999
Richland, WA 99352

L. D. Williams

Sandia Laboratories
P.O. Box 5800
Alburquerque, NM 87115

C. F. Magnuson

Hanford Engineering Development Laboratory (35)
P.O. Box 1970
Richland, WA 99352

c/o Supervisor, Correspondence Processing W/C-123 (35)

AG Blasewitz	W/C-31
DM Bosi	W/A-40
DA Cantley	W/A-40
HA Carlson	W/FED-135
TT Claudson	W/C-16
EA Evans	W/JAD-6
SR Fields (9)	W/FED-135
JF Fletcher	W/FED-135
EM Greene	W/FED-135
LD Jacobson	W/FED-135
RL Knecht	W/A-40
SJ Mech	W/A-132
TE Michaels	W/A-132
WF Sheely	W/C-44
JC Sonnichsen	W/FED-135
JB Yasinsky	W/B-65
Central Files (9)	W/C-110
Publ Services (2)	W/C-115